

## Non-equilibrium compositions of liquid polar stratospheric clouds in gravity waves

Christiane Voigt,<sup>1</sup> Athanasios Tsias,<sup>2</sup> Andreas Dörnbrack,<sup>3</sup> Stefanie Meilinger,<sup>2</sup> Beiping Luo,<sup>2</sup> Jochen Schreiner,<sup>1</sup> Niels Larsen,<sup>4</sup> Konrad Mauersberger,<sup>1</sup> and Thomas Peter<sup>5</sup>

**Abstract.** On 25 January 1998 mountain induced gravity waves developed over Scandinavia leading to the formation of mesoscale polar stratospheric clouds (PSCs). Balloon-borne mass spectrometric measurements of particle composition and optical backscatter measurements were performed above Kiruna/Sweden. PSCs were encountered twice, showing a correlated increase in the condensed phase water, nitric acid and the backscatter ratio. Thermodynamic modeling allows the PSC particles to be unambiguously identified as supercooled ternary solution (STS) droplets, but cannot account for the measured scatter in the particulate  $\text{HNO}_3\text{:H}_2\text{O}$  mole ratio. Simultaneous temperature measurements show that the particles were subject to rapid atmospheric temperature fluctuations of  $\pm 1$  K and cooling/heating rates exceeding 1 K/min caused by the gravity waves. Micro-physical non-equilibrium modeling of STS droplet distributions reveals that the observed temperature perturbations cause particle compositions in close agreement with the measured  $\text{HNO}_3\text{:H}_2\text{O}$  variations. Non-equilibrium compositions of liquid PSC particles are thus a principal stratospheric characteristic related to gravity waves affecting particle evolution.

### Introduction

Soon after the discovery of the ozone hole the fundamental role of polar stratospheric clouds was recognized: heterogeneous reactions on the surface and in the bulk phase of these particles lead to the activation of chlorine and the deactivation of nitrogen oxides as prerequisite for rapid polar ozone destruction. In this process the uptake coefficients for chlorine species depend on composition and phase of the PSCs [Ravishankara and Hanson, 1996]. The cloud particles have been classified in different types. Below the frost point ( $T_{ICE}$ ) type II PSCs containing ice particles can form. Some degrees above  $T_{ICE}$  type I particles can exist, consisting either of solid hydrates of nitric acid (type Ia), e.g. nitric acid trihydrate (NAT) or dihydrate (NAD) [Hanson and Mauersberger, 1988; Worsnop et al., 1993], or of ternary solutions

<sup>1</sup>Max-Planck-Institute for Nuclear Physics, Division of Atmospheric Physics, Heidelberg, Germany

<sup>2</sup>Max-Planck-Institute for Chemistry, Division of Air Chemistry, Mainz, Germany

<sup>3</sup>Institute for Physics of the Atmosphere, DLR Oberpfaffenhofen, Wessling, Germany

<sup>4</sup>Danish Meteorological Institute, Copenhagen, Denmark

<sup>5</sup>Laboratorium für Atmosphärenphysik (LAPETH), ETH Zürich, Switzerland

Copyright 2000 by the American Geophysical Union.

Paper number 2000GL012168.  
0094-8276/00/2000GL012168\$05.00

(type Ib) as suggested by model calculations [Carslaw et al., 1994; Tabazadeh et al., 1994].

The influence of mesoscale temperature fluctuations on phase transitions, enhanced PSC particle formation and subsequent ozone destruction has developed into a major field of investigation [Murphy and Ravishankara, 1994; Eckermann and Preusse, 1999]. The relevance of orographically induced mesoscale waves for non-equilibrium compositions of STS droplet distributions and their potential role in type Ia particle crystallization has been pointed out in model studies [Meilinger et al., 1995; Tsias et al., 1997; Carslaw et al., 1999], while the influence of even smaller scale gravity waves on STS droplet volume was investigated by Bacmeister et al. [1999].

First measurements of reactive nitrogen related to PSCs have been performed in the past by Fahey et al. [1989]. Quantitative measurements of the condensed phase species were reported by Schreiner et al. [1999]. Based on the latter measurements, we focus in this work on the detection of non-equilibrium particle compositions in ternary solution droplets at 3-5.5 degrees above  $T_{ICE}$ . From these measurements we conclude that at temperatures near  $T_{ICE}$  non-equilibrium compositions are a dominant feature of STS clouds and play a role in the analysis of particle measurements and possibly in solid particle formation in the stratosphere.

### Mesoscale meteorological conditions

The meteorological situation above Scandinavia on 25 January 1998 was characterized by leewave activity. Mountain-induced mesoscale stratospheric temperature anomalies had developed due to the adiabatic expansion/compression of ascending/descending air masses. Mesoscale MM5 model simulations [Dörnbrack et al., 1998] show two low temperature regions with a horizontal wavelength of about 250 km and a peak-to-peak amplitude as large as 6 K over northern Scandinavia. Temperatures in the range of 3-7.5 K above  $T_{ICE}$  were measured at the balloon gondola (see Fig. 1), in general agreement with the predictions of the mesoscale model.

Mesoscale trajectory calculations ending at the balloon flight track indicate that the air parcels had experienced temperatures as low as 187 K but still above  $T_{ICE}$ , when passing a hydrostatic mountain wave above the Norwegian mountains 3-5 hours before the measurements. Synoptic scale backtrajectories based on ECMWF-analysis show for the period of 30-240 hours before the encounter temperatures above  $T_{NAT}$ , indicating that the sampled PSC particles had formed in less than 30 hours.

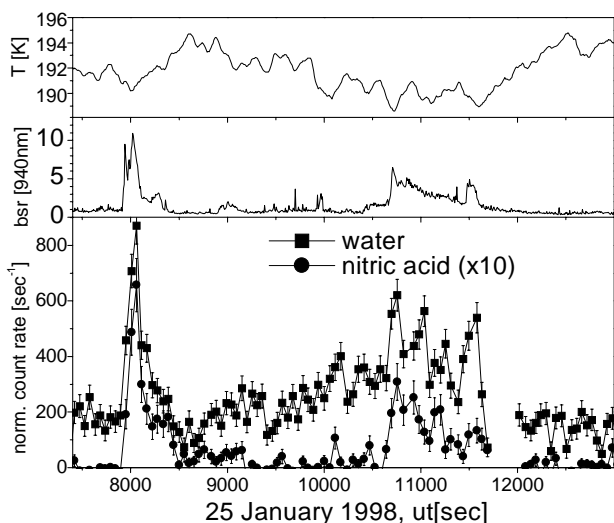


**Figure 1.** ACMS measurements during the balloon flight on 25 January 1998; the normalized count rate of condensed water  $\text{H}_2\text{O}$  (squares) and nitric acid  $\text{HNO}_3$  (times 10, circles), the backscatter ratio at 940 nm and the temperature are plotted versus universal time.

## Measurements

The balloon payload consisted of an aerosol composition mass spectrometer (ACMS) and a backscatter sonde. Particles enter the ACMS through an aerodynamic lens, which focuses the aerosol into a narrow particle beam. Behind the lens gas molecules are differentially pumped by liquid helium pumps. The particles are stopped and evaporated inside a small, heated gold sphere and their composition is measured with a mass spectrometer providing a volume weighted particle composition measurement. The precision (accuracy) of the water measurement is better than 13 % (8 %). The  $\text{HNO}_3:\text{H}_2\text{O}$  mole ratio can be determined with a precision (accuracy) of better than 26 % (33 %).

After reaching a cold layer in 20 km altitude PSCs were encountered twice, identified by a correlated increase in the backscatter ratio [Larsen *et al.*, 2000] and in the mass spectrometer signals for condensed water and nitric acid [Schreiner *et al.*, 1999]. Fig. 1 shows the count rates of condensed water (squares) and nitric acid (times 10, circles) with a temporal resolution of 50 sec, which have been corrected for instrumental differences in the sensitivity of the  $\text{H}_2\text{O}$  and  $\text{HNO}_3$  signals and normalized to the  $\text{H}_2\text{O}$  signal. Between the two PSC encounters an uptake of water into the particles with decreasing temperatures is observed, whereas the nitric acid signal remains below the detection limit. Instrumental background of the ACMS has been determined during the gap in the ACMS data between 11700 and 12000 sec. Backscatter ratios at 940 nm and temperatures are shown in the upper panels. Although the temperature sensor might have an offset of  $\pm 1$  K it is fast enough to resolve temperature fluctuations with a frequency of 0.05 Hz.

## Comparison with STS equilibrium calculations

In Fig. 2 we compare the measured mole concentration of condensed water (per  $\text{cm}^3$  air, circles) with equilibrium

STS model results assuming mixing ratios of 5.5 ppmv  $\text{H}_2\text{O}$ , 10 ppbv  $\text{HNO}_3$  and 0.4 ppbv  $\text{H}_2\text{SO}_4$ . To eliminate the dependence on water partial pressure during the measurements at different altitudes (25–45 mbar), a representation of the data versus the temperature difference to the frost point has been chosen. Although this reference to the frost point reduces the fluctuations in the  $\text{H}_2\text{O}$ - $T$  diagram, the data remain to have a considerable deviations which are not due to particle sampling statistics (more than 20 particles per sample). In addition to the instrumental uncertainties (see error bars) or deviations related to non-equilibrium particle compositions (typically  $\pm 10$  % around the equilibrium curve, calculations not shown), measurements close to the upper edge of the Junge aerosol layer result in changes in condensed phase  $\text{H}_2\text{SO}_4$  as indicated by the gray shaded area (0.2–0.6 ppbv  $\text{H}_2\text{SO}_4$ ). Furthermore, calculations using 8 and 12 ppbv  $\text{HNO}_3$  are shown (dotted lines). The dashed line represents the mole concentration of water in NAT particles per  $\text{cm}^3$  air. Despite the uncertainty in the  $\text{H}_2\text{SO}_4$  the thermodynamic measured uptake of water by the particles is in general agreement with STS model calculations and cannot be explained by NAT particles.

## The influence of temperature fluctuations on particle composition

As displayed in Fig. 1 the temperature exhibits fluctuations of the order  $\pm 1$  K with cooling/heating rates exceeding 1 K/min, which have been measured with two independent temperature sensors. The horizontal wavelength of the temperature oscillations of  $\gtrsim 7$  km is related to the gravity waves and represents the horizontal lower limit of the wavelength of vertically propagating buoyancy waves [Carslaw *et al.*, 1998]. Similar high frequency temperature oscillations have been reported by lidar and satel-

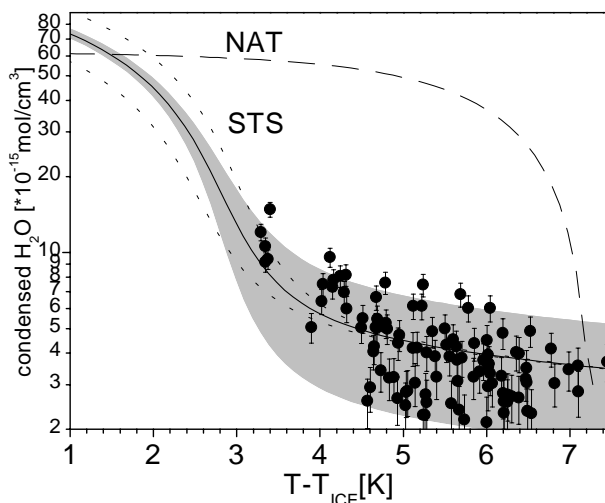


**Figure 2.** Measurements of condensed water (in units  $10^{15}$  mol/ $\text{cm}^3$ , circles) versus temperature difference to the frost point. Solid line: equilibrium STS-calculations using mixing ratios of 5.5 ppmv  $\text{H}_2\text{O}$ , 0.4 ppbv  $\text{H}_2\text{SO}_4$  and 10 ppbv  $\text{HNO}_3$  (8 and 12 ppbv  $\text{HNO}_3$  dotted lines); the boundaries of the gray shaded area are calculated for 0.2 and 0.6 ppbv  $\text{H}_2\text{SO}_4$ . Dashed line: calculated water related to NAT particles. Within the experimental error of  $1\sigma$ , more than 64 % of the data lie within the gray shaded area for STS droplets.

lite measurements [Bacmeister *et al.*, 1999; Eckermann and Preusse, 1999]. To investigate the influence of temperature fluctuations related to gravity waves, we superimposed on MM5 back-trajectories the short wavelength fluctuations experienced by the balloon, which the model cannot resolve. Fig. 3 shows as an example the trajectory for the longer second PSC event. The modified trajectories have been used as input to our non-equilibrium model [Meilinger *et al.*, 1995] and the results are compared to the measurements of particle composition in Fig. 4. Diamonds indicate mole ratios of condensed  $\text{HNO}_3\text{:H}_2\text{O}$  measured within the two PSCs. The solid line represents the calculated equilibrium composition assuming 10 ppbv  $\text{HNO}_3$  (dashed for 8 and 12 ppbv). Altitude-dependent  $\text{H}_2\text{SO}_4$  loadings are indistinguishable from the solid curve in Fig. 4 and cannot account for the scatter in  $\text{HNO}_3\text{:H}_2\text{O}$  mole ratios.  $\text{HNO}_3$  gradients from 4 to 16 ppbv in the same air parcel during a measurement period of 10 (17) minutes in the first (second) PSC would be required to explain the measurements in terms of equilibrium calculations although there is no indication of denitrification in the relatively warm Arctic vortex of the winter 1997/98. Furthermore, the dashed line in Fig. 4 shows that NAT particles cannot explain the data. In contrast, modeled STS droplet compositions, see small crosses in Fig. 4, closely explain the observed factor of 5 scatter in  $\text{HNO}_3\text{:H}_2\text{O}$ , provided that the droplets' non-equilibrium compositions in response to the gravity wave forcing is properly taken into account. The non-equilibrium droplet compositions are caused by the slow uptake of  $\text{HNO}_3$  due to the impedance of the gas phase diffusion with a time constant of 0.5 h, whereas the more abundant water reaches equilibrium between gas and liquid phase (referring to the actual droplet composition) on a time scale of seconds.

Other model runs based directly on the MM5 trajectories without small-scale gravity waves (thick solid curve in Fig. 3) show  $\text{HNO}_3\text{:H}_2\text{O}$  mole ratios differing at most by a factor of 2 and cannot explain a large fraction of the data. Finally, we addressed the possibility that the observed PSCs could consist of mixtures of solid and liquid particles. A typical time constant for the coexistence of NAT and STS

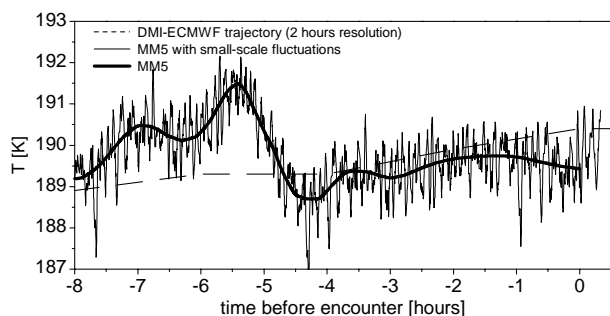


**Figure 3.** Simulated temperature trajectories ending in the second PSC sampled on 25 January 1998 at 10700 sec UT. The nested domain of the mesoscale MM5 simulation (Dörnbrack *et al.*, [1999]) with 12 km horizontal grid size, initialized on 24 January 1998, 12 UT is forced by global analysis in 1.125 x 1.125 degree resolution by the German Weather Service (DWD). Thick curve: MM5 simulation. Dashed curve: ECMWF-DMI trajectory with a temporal resolution of 2 h. Thin line: MM5 trajectory superposed by smallscale T-fluctuations measured at the balloon gondola (Fig. 1).

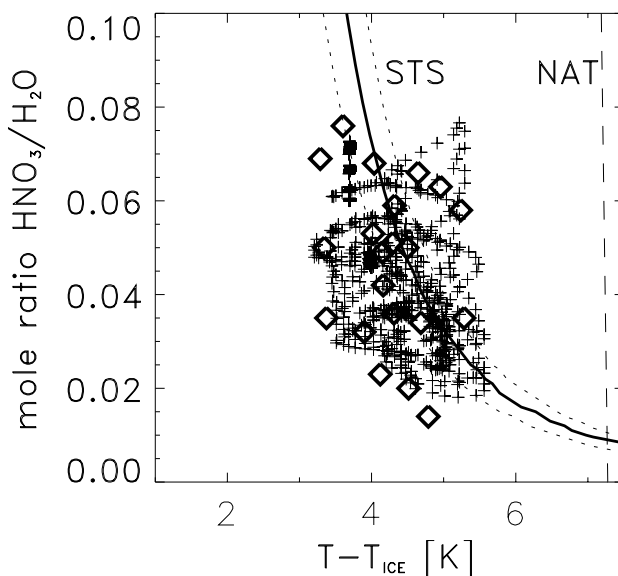


**Figure 4.** Condensed phase nitric acid to water mole ratios versus  $T - T_{\text{ICE}}$ ; Diamonds: measurements during two PSC encounters. Dashed line: equilibrium calculations assuming NAT particles; Solid line: STS equilibrium calculations using mixing ratios of 5.5 ppmv  $\text{H}_2\text{O}$ , 0.4 ppbv  $\text{H}_2\text{SO}_4$  and 10 ppbv  $\text{HNO}_3$  (Dotted lines: 8 and 12 ppbv  $\text{HNO}_3$ ); Small crosses: non-equilibrium model results of the particle composition influenced by temperature oscillations induced by mountain waves.

particles assuming a NAT particle concentration of  $0.1 \text{ cm}^{-3}$  is about 2 hours. Allowing the formation and non-equilibrium evolution of 1 % NAT particles at temperatures below  $T_{\text{NAT}}$  (based on the small scale gravity wave trajectory in Fig. 3), the model results show higher mole ratios and less good agreement with the measurements, indicating that the measured clouds were purely liquid.

## Summary and outlook

Simultaneous measurements of condensed phase  $\text{H}_2\text{O}$  and  $\text{HNO}_3$  are good diagnostics of stratospheric particles subject to gravity waves. The measured  $\text{H}_2\text{O}$  concentration allows the identification of supercooled ternary solution PSCs based on thermodynamic equilibrium calculations. Under the prevalent meteorological conditions, orographically induced mesoscale waves (wave lengths of several 100 km) show a moderate influence on the measured  $\text{HNO}_3$  concentration. Additionally, the  $\text{HNO}_3\text{:H}_2\text{O}$  ratio is strongly influenced by small scale gravity waves (wave lengths of a few km). The observed deviations of the particle composition from thermodynamic equilibrium (up to  $\pm 65\%$ ) can best be explained when temperature fluctuations on both scales are used to force a non-equilibrium STS PSC model. The measurements are thus a direct indication for the dynamical activity of the atmosphere.

**Acknowledgments.** This work has been supported by the Commission of the European Union through the Environment and Climate program (contract ENV4-CT97-0523) and through the Ozone Research Program by the German Federal Government.

## References

- Bacmeister, J.T., et al., Fluctuations induced by a spectrum of gravity waves: A comparison of parameterizations and their impact on stratospheric microphysics, *J. Atm. Sci.*, *56*, 1913-1924, 1999.
- Carslaw, K.S., et al., Stratospheric aerosol growth and HNO<sub>3</sub> gas phase depletion from coupled HNO<sub>3</sub> and water uptake by liquid particles, *Geophys. Res. Lett.*, *21*, 2479-2482, 1994.
- Carslaw, K.S., et al., Particle microphysics and chemistry in remotely observed mountain polar stratospheric clouds, *J. Geophys. Res.*, *103*, 5785-5796, 1998.
- Carslaw, K.S., et al., Widespread solid particle formation by mountain waves in the arctic stratosphere, *J. Geophys. Res.*, *104*, 1927-1836, 1999.
- Dörnbrack, A., et al., Mesoscale forecasts of stratospheric mountain waves, *Meteorol. Appl.*, *5*, 117-126, 1998.
- Dörnbrack, A., et al., Mountain wave induced record low stratospheric temperatures above northern Scandinavia, *Tellus*, *51A*, 951-963, 1999.
- Eckermann, S.D., and P. Preusse, Global measurements of stratospheric mountain waves from space, *Science*, *286*, 1534-1537, 1999.
- Fahey, D., et al., In situ measurements of total reactive nitrogen, total water and aerosol in a polar stratospheric cloud in the Arctic, *J. Geophys. Res.*, *94*, 11,299-11,315, 1989.
- Hanson, D., and K. Mauersberger, Laboratory studies of the nitric acid trihydrate: Implications for the south polar stratosphere, *Geophys. Res. Lett.*, *15*, 855-858, 1988.
- Larsen, N., et al., Comparison of chemical and optical in situ measurements of polar stratospheric cloud particles, *J. Geophys. Res.*, *105*, 1491-1502, 2000.
- Meilinger, S., et al., Size-dependent stratospheric droplet composition in mesoscale temperature fluctuations and their potential role in PSC freezing, *Geophys. Res. Lett.*, *22*, 3031-3034, 1995.
- Murphy, D.M., and A. R. Ravishankara, Temperature averages and rates of stratospheric reactions, *Geophys. Res. Lett.*, *21*, 2471-2474, 1994.
- Ravishankara, A.R., and D.R. Hanson, Differences in the reactivity of type I polar stratospheric clouds depending on their phase, *J. Geophys. Res.*, *101*, 3885-3890, 1996.
- Schreiner, J., et al., Chemical analysis of Polar Stratospheric Cloud particles, *Science*, *283*, 968-970, 1999.
- Tabazadeh, A., R. P. Turco, and M. Z. Jacobson, A model for studying the composition and chemical effects of stratospheric aerosols, *J. Geophys. Res.*, *99*, 12,897-12,914, 1994.
- Tsias, A., et al., Freezing of polar stratospheric clouds in orographically induced strong warming events, *Geophys. Res. Lett.*, *24*, 2303-2306, 1997.
- Worsnop, D., et al., Vapour pressures of solid hydrates of nitric acid: Implication for polar stratospheric clouds, *Science*, *259*, 71-74, 1993.
- 
- K. Mauersberger, J. Schreiner, C. Voigt, Max-Planck-Institute for Nuclear Physics, Division of Atmospheric Physics, P.O.Box 103980, D-69121 Heidelberg, Germany. (e-mail: Christiane.Voigt@mpi-hd.mpg.de, Jochen.Schreiner@mpi-hd.mpg.de, Konrad.Mauersberger@mpi-hd.mpg.de)
- B. Luo, S. Meilinger, A. Tsias, Max-Planck-Institute for Chemistry, Division of Air Chemistry, P.O.Box 3060, D-55020 Mainz, Germany. (e-mail: smeili@mpch-mainz.mpg.de, luo@mpch-mainz.mpg.de)
- A. Dörnbrack, Institute for Physics of the Atmosphere, DLR Oberpfaffenhofen, D-82234 Wessling, Germany. (e-mail: andreas.doernbrack@dlr.de)
- N. Larsen, Danish Meteorological Institute, Division of Middle Atmospheric Research, Lyngbyvej100, DK-2100 Copenhagen, Denmark. (e-mail: niels.larsen@dmi.dk)
- T. Peter, Laboratorium für Atmosphärenphysik (LAPETH), ETH Zürich, Hönggerberg HPP, CH-8093 Zürich, Switzerland. (e-mail: thomas.peter@atmos.unmw.ethz.ch)

(Received August 7, 2000; revised September 19, 2000; accepted September 25, 2000.)